Advanced modeling and trajectory optimization of the in-air-capturing maneuver for winged RLVs

Lâle Evrim Briese, Björn Gäßler

Future reusable launch vehicle concepts and their key technologies have been investigated within the DLR research project AKIRA. In this context, several return options for reusable launch vehicles (RLV) were categorized by vertical (SpaceX, Blue Origin) or horizontal landing strategies (Space Shuttle), and then systematically evaluated based on their influence on overall design and technical feasibility. In general, system dynamics, guidance, and control aspects are of special importance within preliminary design studies, in particular if complex and difficult maneuvers like the DLR-patented in-air-capturing method are considered. In this case, the unpowered winged RLV is captured during descent by an aerodynamically controlled capturing device which is connected to an aircraft by a cable. After successful capturing, the launch vehicle is towed back to its landing site.

In previous studies, the technical feasibility of the in-air-capturing maneuver was mainly assessed by simulations for an aerodynamically controlled RLV and an aircraft which is assumed to be passive. In contrast to this, we consider an optimal control approach to the problem of in-air-capturing, investigating both passive and active (cooperative) RLV and aircraft operations. To study the risk of failure of the in-air-capturing maneuver, both the initial capturing approach and a subsequent second attempt for recapture after an initial miss are analyzed. For this purpose, a multi-disciplinary multibody modeling and simulation framework based on the object-oriented modeling language MODELICA is used for the consistent flight dynamics modeling of each vehicle including a rigid cable connecting the aircraft and its capturing device. The trajectory optimization results provide an overview of the dynamic behavior of the multibody system for several constraints and flight conditions. Additionally, the results show that for a successful in-air-capturing maneuver with minimum control effort and multiple recapturing attempts, an actively controlled aircraft with drag-increasing subsystems and a cooperative launch vehicle maintaining a suitable flight path angle are recommended. The obtained reference trajectories can be used for future controllability studies and control system design considering a flexible cable and disturbances.

Lâle Evrim Briese, Björn Gäßler: Advanced modeling and trajectory optimization of the in-air-capturing maneuver for winged RLVs, Acta Astronautica, 2021, ISSN 0094-5765, https://doi.org/10.1016/j.actaastro.2021.09.005.

Advanced Modeling and Trajectory Optimization of the In-Air-Capturing Maneuver for Winged RLVs*

Lâle Evrim Briese*, Björn Gäßler

DLR, German Aerospace Center
Institute of System Dynamics and Control
D-82234 Oberpfaffenhofen, Germany

Abstract

Future reusable launch vehicle concepts and their key technologies have been investigated within the DLR research project AKIRA. In this context, several return options for reusable launch vehicles (RLV) were categorized by vertical (SpaceX, Blue Origin) or horizontal landing strategies (Space Shuttle), and then systematically evaluated based on their influence on overall design and technical feasibility. In general, system dynamics, guidance, and control aspects are of special importance within preliminary design studies, in particular if complex and difficult maneuvers like the DLR patented in-air-capturing method are considered. In this case, the unpowered winged RLV is captured during descent by an aerodynamically controlled capturing device which is connected to an aircraft by a cable. After successful capturing, the launch vehicle is towed back to its landing site.

In previous studies, the technical feasibility of the in-air-capturing maneuver was mainly assessed by simulations for an aerodynamically controlled RLV and an aircraft which is assumed to be passive. In contrast to this, we consider an optimal control approach to the problem of in-air-capturing, investigating both passive and active (cooperative) RLV and aircraft operations. To study the risk of failure of the in-air-capturing maneuver, both the initial capturing approach and a subsequent second attempt for recapture after an initial miss are analyzed. For this purpose, a multi-disciplinary multibody modeling and simulation framework based on the object-oriented modeling language MODELICA is used for the consistent flight dynamics modeling of each vehicle including a rigid cable connecting the aircraft and its capturing device. The trajectory optimization results provide an overview of the dynamic behavior of the multibody system for several constraints and flight conditions. Additionally, the results show that for a successful in-air-capturing maneuver with minimum control effort

*Presented at the 71st International Astronautical Congress (IAC) – The CyberSpace Edition, October 12-14, 2020.

*Corresponding author.

Email addresses: lale.briese@dlr.de (Lâle Evrim Briese), bjoern.gaessler@dlr.de (Björn Gäßler)

and multiple recapturing attempts, an actively controlled aircraft with drag-increasing subsystems and a cooperative launch vehicle maintaining a suitable flight path angle are recommended. The obtained reference trajectories can be used for future controllability studies and control system design considering a flexible cable and disturbances.

Keywords: multibody modeling, trajectory optimization, in-air capturing maneuver, flight dynamics, reusable launch vehicles, launch vehicle system dynamics

---

1. Introduction

The investigation of technically feasible and financially viable return options is imperative for the assessment and development of future reusable launch vehicle concepts and technologies. The overall design of reusable launch vehicle systems is closely linked to the chosen return option – especially when the launch vehicle is recovered fully or only partially. As a consequence, a systematic evaluation of possible return concepts and their influence on the launch vehicle system is already required in early launch vehicle design phases, such as the preliminary design phase. These early assessments including system dynamics, guidance, and control aspects are of particular importance within preliminary design studies, especially if complex and difficult maneuvers like the DLR-patented in-air-capturing method [1, 2] are considered.

Over the past years, several return concepts for fully or partially reusable launch vehicles have been investigated by the DLR research project Akira [3] focusing on the comparison and systematic evaluation of key technologies [4, 5]; be they realized by vertical landing (e.g. SpaceX [6], Blue Origin [7]) or horizontal landing (e.g. Space Shuttle [8]). In this context, the in-air-capturing maneuver for unpowered winged first stages of reusable launch vehicles has been studied in terms of flight dynamics and sub-scale flight tests. The operational concept, feasibility, potential performance advantage, and main challenges of the in-air-capturing maneuver are discussed in detail in [1, 9, 10, 11, 12], while [13, 14, 15] focus on sub-scale flight tests.

As illustrated in Figure 1, the in-air-capturing maneuver in principle involves three flight vehicles - an unpowered winged first stage of a vertical takeoff and horizontal landing (VTHL) launch vehicle system in a two-stage-to-orbit (TSTO) configuration, an aircraft which is supposed to tow the first stage to its landing site, and a capturing device which is connected to the aircraft by a cable. After stage separation, the first stage performs a ballistic trajectory and subsequent reentry into the atmosphere. During the descent phase, the first stage loses altitude rapidly, hereby maintaining a steep flight path angle. Consequently, since the first stage is unpowered, it is not able to fly back to the launch site independently. Therefore, a modified aircraft awaits the returning first stage at an appropriate cruise flight altitude while a highly agile aerodynamically controlled capturing device is deployed from the aircraft by a cable. The main task of the aerodynamically controlled capturing device is to actively pursue a

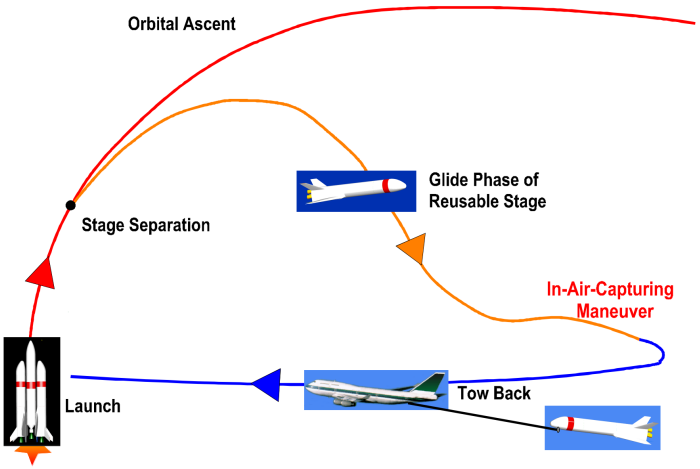

Figure 1: Schematic overview of the in-air-capturing maneuver [9].

capturing maneuver of the first stage. After the in-air-capturing maneuver, the reusable first stage is towed back to the landing site by the autonomous aircraft. Close to the landing site, the unpowered winged first stage is released from the capturing device and autonomously glides to the landing runway [15].

Current return concepts such as *return to launch site* (RTLS) or *down-range landing* (DRL) require significant amounts of return propellant and possibly an additional propulsion system for descent and landing maneuvers as discussed in [4, 5, 16]. Recovering the first stage by an in-air-capturing maneuver has the advantage that the downrange of the burned-out first stage can be increased while no additional propellant has to be allocated for the return flight. Therefore, the in-air-capturing method can offer a performance advantage due to the first stage's lower inert mass compared to alternative return options as highlighted in [4, 5]. However, the in-air-capturing maneuver can be challenging, since multiple flight vehicles with different flight dynamics are involved in a cooperative flight maneuver while being exposed to external disturbances and uncertainties. For instance, the aerodynamic controllability of the aircraft with a high lift-to-drag ratio is bound to time delays while the winged first stage with a relatively low lift-to-drag ratio maintains a steep nose dive during descent as discussed in [9]. Additionally, the capturing process is limited to a short time window of approximately two minutes.

Consequently, for such a demanding maneuver involving multiple vehicles with highly dynamic flight behavior, it is imperative to consider all relevant system dynamics and control aspects already in the preliminary design phase. Most importantly, it is necessary to characterize the trajectory of all vehicles and attachments (e.g. cable and capturing device) to assess the feasibility of the overall concept. However, in previous trajectory optimization concepts as described in [9], this maneuver was mainly assessed focusing on the aircraft and

launch vehicle interaction. For instance, it was assumed in these studies, that the aircraft remains in a passive mode at cruise flight altitude with the same flight path azimuth angle until a certain distance and angle threshold between both vehicles is reached. Thereupon, the aircraft matches the flight path angle of the launch vehicle such that both vehicles glide along the same trajectory while maintaining an appropriate distance to enable multiple capturing attempts.

In contrast to this, we consider an optimal control approach to the in-air-capturing problem, investigating both passive and active (cooperative) launch vehicle operations. To study the risk of failure of the in-air-capturing maneuver both the initial capturing approach and a subsequent second attempt for recapture after an initial miss are analyzed. For this purpose, a multi-disciplinary multibody modeling and simulation framework based on the object-oriented modeling language Modelica is used for the consistent flight dynamics modeling of each vehicle including a rigid cable. The trajectory optimization results showcase the dynamic behavior of the multibody system for several constraints and flight conditions.

The objective of this paper is to present the key elements of the in-air-capturing modeling approach and the results of the trajectory optimization considering all flight vehicles involved. After introducing the modeling framework in Section 2, the implementation of each flight vehicle and the trajectory optimization constraints and requirements are presented in Section 3. Finally, the results of the trajectory optimization are discussed in Section 4 and 5.

2. Modeling Approach

The modeling of multiple flight vehicles within one consistent simulation setup specifically for trajectory optimization can be a challenging task due to performance requirements in terms of computational effort and model complexity, as well as due to the highly interconnected disciplines involved in the problem statement, such as propulsion, aerodynamics, structural dynamics, separation or contact dynamics, amongst others. In particular, changing environmental conditions and perturbations have to be considered throughout the simulation to guarantee an accurate and consistent modeling approach.

However, for preliminary design studies involving complex mission scenarios, such as the in-air-capturing maneuver, the general problem is often simplified. In particular, the cable attached to the aircraft and its capturing device are often not considered for trajectory optimization as described in [9]. Within the DLR internal project Akira, the research task was to incorporate all relevant flight vehicles, namely the launch vehicle (LV), the aircraft (AC), its capturing device (CD), as well as the cable between aircraft and capturing device, into one simulation framework to assess the feasibility of the maneuver. For this purpose, the multi-domain modeling language Modelica was used to address the multibody modeling requirements of multiple flight vehicles within one simulation setup.

Modelica as a modern object-oriented and equation-based modeling language is widely used for applications in aeronautics, automotive, or robotics,

where the modeling of complex physical systems containing, e.g., mechanical, electrical, control, or process-oriented subsystems and components becomes increasingly important [17, 18, 19]. In general, MODELICA models can be described using differential, algebraic, and discrete equations which are mapped into Differential Algebraic Equations (DAE) or Ordinary Differential Equations (ODE) by reordering the derivatives and algebraic variables. These equations can then be solved and simulated by MODELICA-based simulation environments such as DYMOLA [20]. In contrast to imperative languages, MODELICA is declarative, meaning that equations do not specify a certain data flow direction which is one of the major advantages of this language as discussed in [21, 22].

Over the past years, DLR's *Institute of System Dynamics and Control* (SR) has been developing MODELICA-based libraries for object-oriented and multi-disciplinary multibody modeling and simulation covering a wide scope of applications, such as flight vehicle dynamics [23, 24], satellite dynamics [25], on-orbit servicing with a robotic arm [26], and separation dynamics of launch vehicle stages [27]. More recently, a multi-disciplinary multibody modeling and simulation framework for launch vehicle systems has been introduced in [21, 22]. For instance, launch vehicle multibody models used in this framework can be extended, exchanged and reused for different purposes such as trajectory optimization, performance studies, or control system design. This object-oriented approach enables modularized models to meet analysis-specific requirements in one single simulation environment, thus guaranteeing numerical consistency, amongst others. Consequently, this framework was used as a baseline for the modeling of the in-air-capturing scenario as discussed more in detail in [12]. The main contributing MODELICA-based libraries are listed below:

- Modelica Standard Library [17, 28]
  This library provides basic multi-physical models, ranging from signal-based control blocks to equation-based multibody models underlining MODELICA's multi-domain modeling capabilities. Within its *MultiBody* package, generic body components are defined by physical properties such as constant mass and moments of inertia. Their translational and rotational dynamics are described internally by the *Newton-Euler* equations of motion. In order to characterize the interaction between multiple bodies, *frames* are assigned to each body which contain their position, orientation, cut-forces, and cut-torques. The physical coupling between multiple bodies can be ideally constrained by simply connecting their frames with each other, whereas *joints* can be used to apply motion constraints between two bodies (see Section 2.1).

- DLR Environment Library [29]
  This library provides components for the modeling of environmental effects which are associated with different planet types, coordinate systems, gravity, atmosphere, wind, and disturbance models. However, for the trajectory optimization of the in-air-capturing maneuver the *Earth Gravitational Model 1996* [30] and the *U.S. Standard Atmosphere 1976* [31] are used, whereas wind and disturbances are neglected.

- DLR LauncherApplications Library [21, 22, 32]
  The system dynamics modeling and simulation framework for guidance and control applications enables the multi-fidelity modeling of launch vehicle systems which can be easily adapted to different flight vehicles and mission requirements. Application-specific models and interfaces to other tools like the trajectory optimization package *trajOpt* are available. In this paper, simplified three degrees of freedom (DOF) models are used for trajectory optimization. However, as highlighted in [12, 22], these models can be extended almost effortlessly to corresponding 6-DOF flight dynamics models considering structural elastic effects for subsequent controllability and performance studies.

2.1. In-Air-Capturing Model

A schematic overview of the in-air-capturing modeling approach is depicted in Figure 2 for a planar scenario. The equivalent object-oriented multibody representation of this schematic overview is shown in Figure 3, while the description of the external input parameters can be retrieved from Table 1. In both overviews, all three flight vehicles including the rigid cable between the aircraft and its capturing device are illustrated.

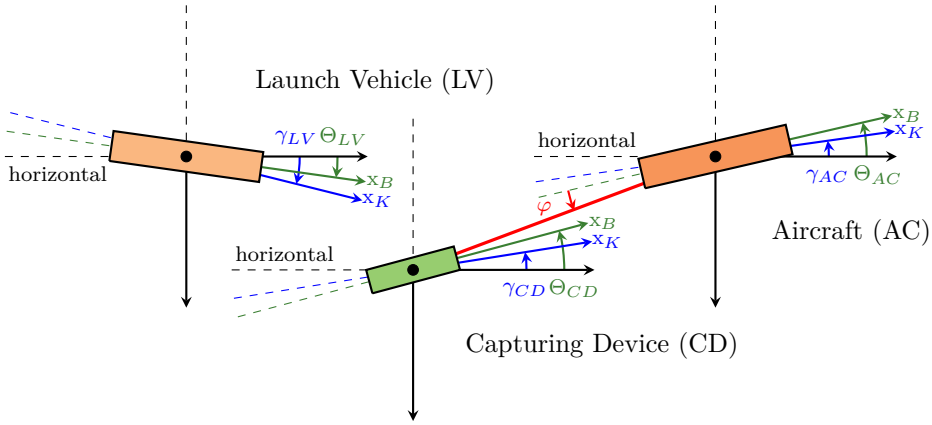

Figure 2: Simplified schematic overview of the in-air-capturing model.

As indicated by the red thick line in Figure 2, the cable is connected to the aircraft with an initial angle φ around the aircraft's y-axis with respect to its body-fixed coordinate system. For the trajectory optimization, the motion constraint between the aircraft and the cable is assumed to be represented by a spherical multibody joint to enable free rotation around the attachment point which in turn results in a free movement of the capturing device depending on its control inputs and the aircraft's flight dynamics. The angle φ is used to initialize the capturing device's relative position to the aircraft and to enforce the capturing device to remain below the xy-plane of the aircraft with respect

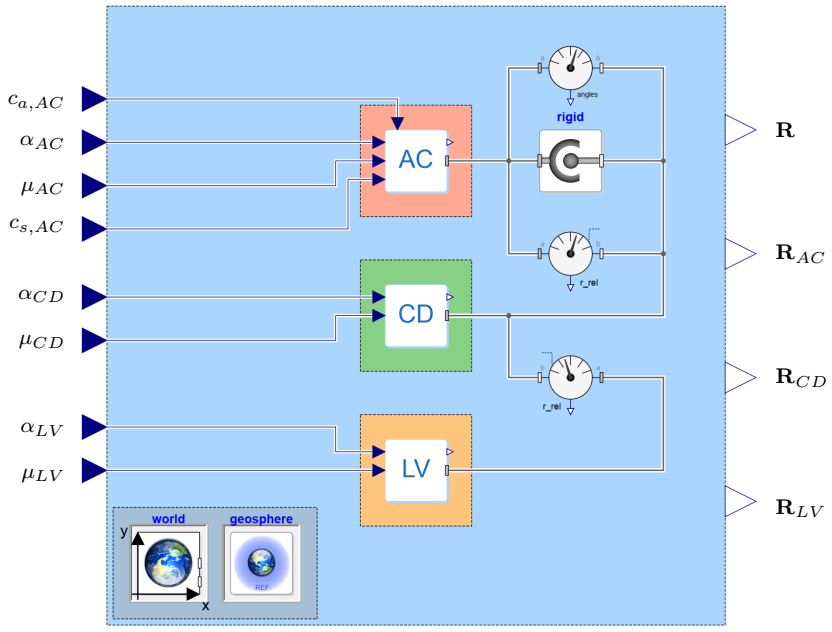

Figure 3: In-air-capturing multibody model in MODELICA.

Table 1: Input parameters of the in-air-capturing model.

Vehicle Type	Variable	Description
Aircraft	$c_{a,AC}$	Drag Scaling Factor
	α_{AC}	Angle of Attack
	μ_{AC}	Bank Angle
	$c_{s,AC}$	Throttle Factor
Capturing Device	α_{CD}	Angle of Attack
	μ_{CD}	Bank Angle
Launch Vehicle	α_{LV}	Angle of Attack
	μ_{LV}	Bank Angle

to its body-fixed coordinate system by constraining φ to positive values. This constraint is necessary to avoid unphysical overlapping between the cable and the aircraft's body since all flight vehicles are modeled as 3-DOF point masses without geometric properties. Consequently, a negative angle φ would mean that the cable crosses the aircraft's body boundaries. Furthermore, the orientation of the capturing device remains independent from the cable's attitude at its attachment point as depicted in Figure 2 by the body-fixed coordinate system of the capturing device indicated by x_B.

The MODELICA-based top-level multibody model shown in Figure 3 contains dedicated flight dynamics models for each flight vehicle as indicated by AC, CD and LV. These simplified 3-DOF flight dynamics models include several submodels corresponding to disciplines such as aerodynamics and propulsion using an object-oriented approach. For instance, inside an *aerodynamics* submodel aerodynamic forces can be derived from multi-dimensional aerodynamic databases, while an *engine* submodel can be used to calculate and apply thrust forces if required. Additional information regarding the internal flight vehicle architecture, the modified *Newton-Euler* equations of motion for variable mass dynamics, as well as detailed kinematics and dynamics formulations can be obtained from [12, 21, 22] for a single launch vehicle modeling approach.

In contrast to a single launch vehicle model, the complete in-air-capturing model consists basically of two model layers – the top-level environment layer shown in Figure 3 where all flight vehicles are located, as well as the flight vehicle dependent model layer on subsystem level. The top-level environment layer contains the *world* and *geosphere* components [29], which declare the inertial and rotating reference coordinate systems, as well as provide the gravitational and atmospheric models. These top-level environment models can be referenced from inside the flight vehicle models which means that all flight vehicles are subjected to the same environment formulation depending on each flight vehicle's own position and attitude.

In addition to the environment and flight vehicle models, further problem specific components can be included into the top-level layer. For instance, sensors measuring the relative distance, velocity, angle or angular velocity between two frames, are provided already by the *Modelica Standard Library* and can be physically attached to the corresponding flight vehicles. In Figure 3, sensors between the launch vehicle and the capturing device with respect to the launch vehicle's body-fixed coordinate system, and between the capturing device and the aircraft with respect to the capturing device's body-fixed coordinate system are used for the measurement of relative distance and velocity. Additionally, a sensor is included to measure the relative angle between the aircraft's and the cable's body-fixed coordinate system. However, the sensor measurements in this paper are performed with respect to each flight vehicle's center of mass without considering the sensor positions or geometric shapes of the vehicles.

Furthermore, the external output vectors $\mathbf{R}$, $\mathbf{R}_{AC}$, $\mathbf{R}_{CD}$, and $\mathbf{R}_{LV}$ collect all quantities, such as positions, velocities, accelerations, and load factors for each flight vehicle. These quantities can be used by the trajectory optimization to evaluate the performance and flight dynamics behavior of each flight vehicle separately.

3. Implementation

In this chapter, the implementation of the flight vehicles and components involved in the in-air-capturing maneuver shown in Figure 3 will be discussed. Finally, the control parameters, capturing conditions and path constraints defined by the trajectory optimization setup will be presented.

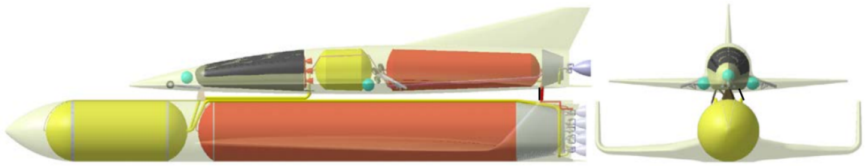

Figure 4: Sketch of the SpaceLiner configuration [33].

Table 2: Initialization parameters of the launch vehicle.

Parameter	Value	Unit
Altitude (geocentric)	10000	m
Latitude (geocentric)	8	deg
Longitude	−49	deg
Flight Path Velocity	214	m/s
Flight Path Angle	−14	deg
Flight Path Azimuth Angle	90	deg
Total Mass (constant)	214000	kg

3.1. Launch Vehicle (LV)

The SpaceLiner concept illustrated in Figure 4 has been developed at DLR's *Institute of Space Systems* (RY) as discussed in [33, 34]. The two-stage-to-orbit launch vehicle configuration is based on a fully reusable, vertical takeoff and horizontal landing approach with a winged reusable booster stage located underneath a winged reusable ascent stage. The chosen propellant combination for each stage is LOX/LH2. A typical target orbit for the SpaceLiner configuration is a Geostationary Transfer Orbit (GTO) with a desired payload of more than 8 t. However, the reference trajectory in this paper targets a Sun-Synchronous Orbit (SSO), where only the in-air-capturing phase during the descent of the booster stage will be investigated.

The initialization parameters defined in Table 2 are derived from the reference trajectory for a 'best-glide' configuration provided by DLR-RY. The aerodynamically controlled and unpowered launch vehicle is implemented as a 3-DOF flight dynamics model with constant mass. The translational states are the geocentric latitude, longitude, and radius, and the velocity vector with respect to the *North-East-Down* (NED) coordinate system as discussed in [21, 22]. The aerodynamic lift and drag coefficients are computed by the *aerodynamics* submodel of the booster stage and depend on the aerodynamic angle of attack and Mach number of the vehicle. The external control inputs of the launch vehicle model are the aerodynamic angle of attack α_{LV} and the aerodynamic bank angle μ_{LV} as shown in Table 1. Additionally, the aerodynamic sideslip

angle β_{LV} is nominally kept at 0°, but can also be used as a control input if required.

3.2. Aircraft (AC)

In this paper, the aircraft is assumed to be similar to a large carrier aircraft like a Boeing 747-400 with an approximate mass of 210 000 kg at the start of the in-air-capturing maneuver and a maximum sea level thrust of approximately 270 kN for each of its four engines. The aircraft is implemented as a 3-DOF flight dynamics model based on the same states and model architecture used for the launch vehicle. Since the in-air-capturing maneuver is performed in a short time window, the variable mass dynamics of the aircraft due to the fuel flow rate are neglected. Additionally, the aircraft model contains an *engines* submodel which computes and applies the total available thrust to the center of mass of the aircraft. The total thrust can be scaled by the throttle factor $c_{s,AC}$ within an operating range of 5 % to 100 %.

Furthermore, the translational aerodynamic coefficients for this configuration provided by DLR-RY depend also on the angle of attack and the Mach number. However, a drag scaling factor $c_{a,AC}$ can be applied to the nominal aerodynamic drag coefficient of the complete aircraft to represent the influence of additional drag induced by air brake systems, which are required for multiple capturing attempts (see Section 4.2). Similar to the launch vehicle, the aircraft is aerodynamically controlled by the aerodynamic angle of attack α_{AC} and the aerodynamic bank angle μ_{AC}, whereas the aerodynamic sideslip angle β_{AC} is neglected.

3.3. Capturing Device (CD)

The capturing device as discussed in [13, 14, 16] and shown in Figure 5 is a highly agile, aerodynamically controlled, unpowered flight vehicle with an overall mass of approximately 135 kg. The multibody model of the capturing device is implemented similarly to the launch vehicle model in terms of subsystem components. Since the capturing device is unpowered as well, the *engines* component and consequently a throttle factor are not required. The position, velocity, and overall flight performance of the capturing device depend primarily on the dynamic behavior of the aircraft. However, due to its own aerodynamic control surfaces and its attachment to the cable by a modified spherical joint, the capturing device is able to pursue small maneuvers in order to capture the launch vehicle during final approach. Therefore, the external control inputs are the aerodynamic angle of attack α_{CD} and the aerodynamic bank angle μ_{CD}.

The capturing device is connected to the aircraft by a steel cable with an overall length of 300 m. To reduce the computational effort regarding the trajectory optimization, the cable is implemented as a massless translational element which incorporates only rigid multibody dynamics, whereas in [12] the rigid cable is replaced by a beam-based flexible multibody model. The aim of this simplification is to relate the translational states of the capturing device to the aircraft considering a fixed distance of 300 m, while enabling capturing maneuvers

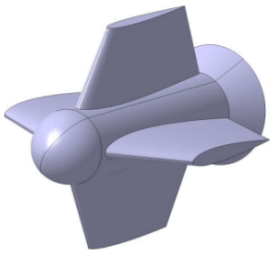

Figure 5: Overview of a preliminary capturing device design [35].

using the aerodynamic control surfaces of the capturing device. Furthermore, the aerodynamic drag coefficient of the cable is approximated for a generic cylindrical shape and applied to the rigid element. Since the capturing itself is described by mathematical conditions and not simulated during the trajectory optimization using contact dynamics models, compressive forces are not transmitted by the cable.

3.4. Trajectory Optimization

The trajectory optimization of the in-air-capturing maneuver is performed by DLR-SR's *Multi-Objective Parameter Synthesis* toolbox MOPS and its trajectory optimization package *trajOpt* as discussed in [21, 36, 37, 38]. For this purpose, the multibody model shown in Figure 3 is exported as a tool-independent *Functional Mock-up Unit* (FMU) for model exchange as defined in [39]. The FMU is used to access and simulate the model by the MATLAB-based trajectory optimization package *trajOpt*. A similar process including multiple FMU models is described in detail within [21]. After the definition of problem-specific optimization criteria, tuning parameters, and constraints, the multi-objective trajectory optimization problem can be solved using standard nonlinear programming (NLP) methods supported by MOPS.

All optimization cases in Section 4 share a common set of controls and control limits provided in Table 3 which relate to the input parameters of the multibody model in Figure 3 and the angle of attack limits of each flight vehicle. Fixing the bank angle for all vehicles effectively constrains the maneuver to the vertical plane which still covers all relevant flight dynamics aspects regarding altitude and speed variations. The final capturing conditions between the capturing device and the launch vehicle are defined in Table 4. These mathematical conditions state that the flight path of the capturing device and the launch vehicle must be aligned for a successful capturing, while maintaining a small distance. Additionally, the launch vehicle must approach the capturing device from behind at a low relative velocity, which corresponds to the negative relative velocity defined in Table 4. This condition is secured by requiring the velocity of the capturing device to be smaller than that of the launch vehicle when aligned. The path constraints stated in Table 5 regarding the flight path angle, dynamic

Table 3: Control parameters.

Description	Bounds
Drag Scaling Factor	$c_{a,AC} \in [1,\ 4.5]$
Throttle Factor	$c_{s,AC} \in [0.05, 1]$
Angle of Attack (AC)	$-5^\circ \leq \alpha_{AC} \leq 12^\circ$
Angle of Attack (CD)	$-20^\circ \leq \alpha_{CD} \leq 20^\circ$
Angle of Attack (LV)	$-5^\circ \leq \alpha_{LV} \leq 15^\circ$
Bank Angle (AC)	μ_{AC} fixed at 0°
Bank Angle (CD)	μ_{CD} fixed at 0°
Bank Angle (LV)	μ_{LV} fixed at 0°

Table 4: Capturing conditions.

Description	Mathematical Condition
Flight Path Angle	$\gamma_{CD} - \gamma_{LV} \in [-1^\circ, 1^\circ]$
Flight Path Azimuth	$\chi_{CD} - \chi_{LV} \in [-1^\circ, 1^\circ]$
Distance	$r_{CD,LV} \leq 2\,\mathrm{m}$
Distance Change	$\lvert\dot{r}_{CD,LV}\rvert \leq 2\,\mathrm{m/s}$
Flight Path Velocity	$v_{CD} - v_{LV} < 0\,\mathrm{m/s}$

Table 5: Path constraints.

Description	Mathematical Condition
Flight Path Angle	$\gamma_{AC} \in [-20^\circ, 20^\circ]$
Dynamic Pressure	$q_{AC} \leq 20\,\mathrm{kPa}$
Normal Acceleration	$n_{z,AC} \leq 3.0$
Normal Acceleration	$n_{z,LV} \leq 4.0$
Angle (AC, Cable)	$\varphi_{AC,cable} > 0^\circ$

pressure and normal acceleration of the aircraft are derived from [15], amongst others. However, during the trajectory optimization, the maximum dynamic pressure and normal acceleration of the aircraft remain well below the chosen limits. Furthermore, the angle $\varphi_{AC,cable}$ between the cable and the xy-plane of the aircraft with respect to its body-fixed coordinate system is constrained to positive values as described in Section 2.

Within the trajectory optimization package *trajOpt* the system's differential equations can be mathematically described for each of its phases j as an initial value problem of the form

$$\dot{x}^j = f^j(t, x^j, u^j, p^j), \quad x^j(t^{j-1}) = s^j, \quad j \in 1 \ldots m \tag{1}$$

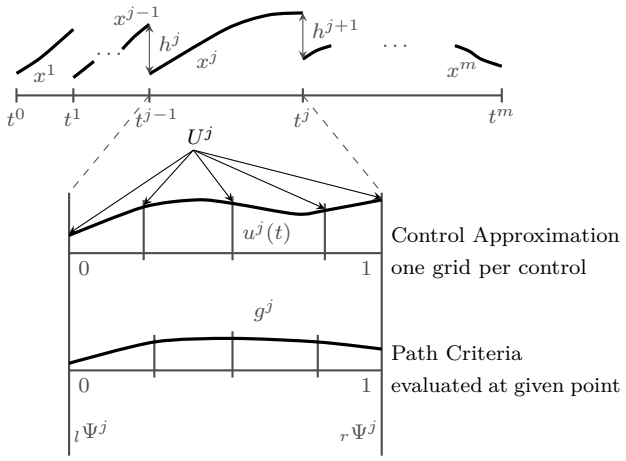

Figure 6: Multi-phase trajectory optimization problem with control discretization [21, 38].

with possibly optimizable phase times

$$t^j \in \{t^0 < t^1 < \ldots < t^m\} \tag{2}$$

where m is the total number of phases, $x^j(t)$ are the system's states for each phase j, $u^j(t)$ are optimizable control functions, p^j are constant scalar modeling parameters, and s^j are the initial values. Phases are then connected by dedicated phase connect constraints h^j as described in [21, 38]. For each phase j optimization criteria Ψ can be defined at the phase's initial and final time as well as by optional path criteria g^j evaluated at discrete times within the phase. These criteria can be specified as a set of minimum, equality or inequality criteria as discussed in [21, 37, 38]. Figure 6 shows a graphical representation of the general optimization problem with m phases, including the control approximation and path criteria formulation. The control functions are discretized by approximation functions (e.g. piecewise polynomial functions) which are dependent on the optimization parameters / tuners of the optimization problem.

Finally, k design objectives can be defined as positive criteria c_k which have to be minimized against their corresponding demanded values d_k, while considering the following min-max constrained multi-criteria optimization problem (see MOPS [37]):

$$\min_{\mathcal{T}} \left\{ \max_{k \in S_m} \left\{ \frac{c_k(\mathcal{T})}{d_k} \right\} \right\}, \tag{3a}$$

$$\begin{aligned} \text{subject to } c_k(\mathcal{T}) &= d_k, \quad k \in S_\text{e}, \\ c_k(\mathcal{T}) &\leq d_k, \quad k \in S_\text{i}, \end{aligned}$$

with:

$$\mathcal{T}_\text{min} \leq \mathcal{T} \leq \mathcal{T}_\text{max}. \tag{3b}$$

Here, S_m is the set of criteria to be minimized, S_e is the set of equality constraints and S_i is the set of inequality constraints; $\mathcal{T}$ is a vector containing the optimization parameters with its upper and lower bounds $\mathcal{T}_\mathrm{min}$ and $\mathcal{T}_\mathrm{max}$.

For the in-air-capturing maneuver, the problem formulation simplifies to a single phase with an optimizable phase final time. In order to specify a well-defined optimization problem, the integrals of the square of the control inputs are used as cost functionals which have to be minimized while simultaneously fulfilling the inequality constraints for capturing conditions and path criteria as stated in Tables 4 and 5. During the initial in-air-capturing maneuver (see Section 4.1) only the control efforts regarding the angle of attack of the launch vehicle, aircraft, and capturing device are used. However, for the passive launch vehicle case, the corresponding cost function for the launch vehicle's control effort is neglected. For the recapturing attempt as discussed in Section 4.2 the weighted sum of the control efforts regarding the drag scaling factor and the throttle factor are included. Additionally, the overall control effort defined as the sum of each cost functional is minimized during the initial in-air-capturing maneuver and the recapturing attempt. Figure 7 shows an example for the initial control approximation as well as the optimized control inputs for the aircraft's angle of attack and throttle factor. As depicted in Figure 7, for each control discretization a dedicated control grid can be defined within the same phase.

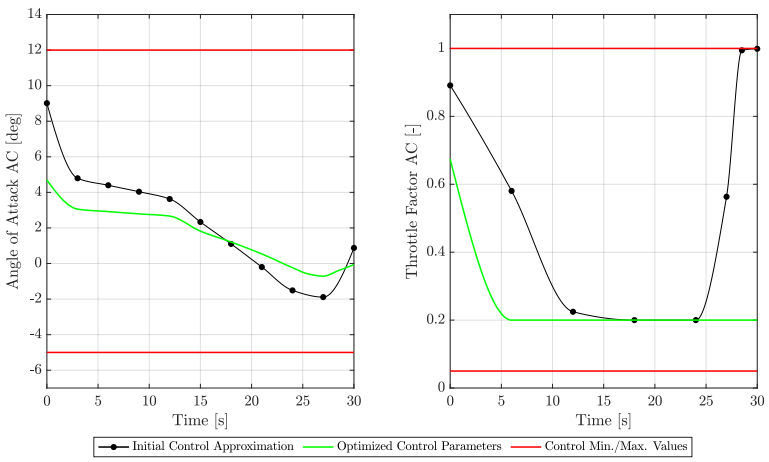

Figure 7: Control approximation of the aircrafts's angle of attack and throttle factor compared to the optimized control parameters with minimum and maximum allowed values.

4. Results & Discussion

Within this section, the trajectory optimization results of the overall in-air-capturing maneuver are discussed based on Figures 8, 9 and 10. As mentioned in the previous chapter, these results are provided for two decoupled flight phases

– namely, the initial in-air-capturing maneuver and a subsequent recapturing maneuver after a possible unsuccessful initial capturing attempt. For all cases, the trajectory optimization results include the altitude, flight path velocity, flight path angle and angle of attack of the aircraft, its capturing device, and the launch vehicle. The throttle scaling factor $c_{s,AC}$ and the drag scaling factor $c_{a,AC}$ are also provided for the aircraft. In order to assess the capturing conditions, the absolute distance, the distance change rate and the velocity difference between the capturing device and the launch vehicle are shown.

4.1. Initial Capturing Maneuver

For the initial in-air-capturing maneuver, only the final flight phase before the in-air-capturing attempt with an overall duration of approximately 20 s to 30 s is considered. This flight phase focuses on the approach of the launch vehicle to the aircraft with the already deployed capturing device up to a first viable capturing position as defined by the capturing conditions in Table 4. However, this flight phase does not consider the deployment of the capturing device, the transient contact between the capturing device and the launch vehicle or any previous flight maneuvers of both vehicles to reach the required initial conditions. Therefore, two basic scenarios are investigated:

- Passive Launch Vehicle
  In this case, the unpowered launch vehicle remains passive throughout the in-air-capturing maneuver and basically follows a 'best-glide' path with a constant angle of attack and a steep flight path angle. The aircraft and its capturing device have to perform maneuvers to match the launch vehicle's flight path and to enable the rendezvous between the capturing device and the launch vehicle under suitable capturing conditions. This reference scenario is used to evaluate the performance of the in-air-capturing concept.

- Active / Cooperative Launch Vehicle
  In this scenario, the launch vehicle actively cooperates with the aircraft and its capturing device by deviating from its 'best-glide' path in order to provide a higher altitude and a less steep flight path angle for the capturing attempt. This is a cooperative maneuver scenario that should lead to more favorable flight conditions for the initial capturing and possible subsequent recapturing attempts.

For both scenarios of the initial capturing maneuver, the launch vehicle is initialized using the 'best-glide' flight conditions defined in Table 2. For the aircraft and its capturing device, the initialization requires level flight conditions ($\gamma_{AC} \approx 0°$) with matching flight path azimuth angles and flight path velocities as depicted in Figures 8 and 9. Apart from these conditions, the remaining initial states are determined by the optimization process. In these scenarios, the drag scaling factor $c_{a,AC}$ is not active as a control input.

As indicated in Figures 8 or 9 for Case 1, the optimal solution for the aircraft is to approach the launch vehicle from below with an excess velocity with respect

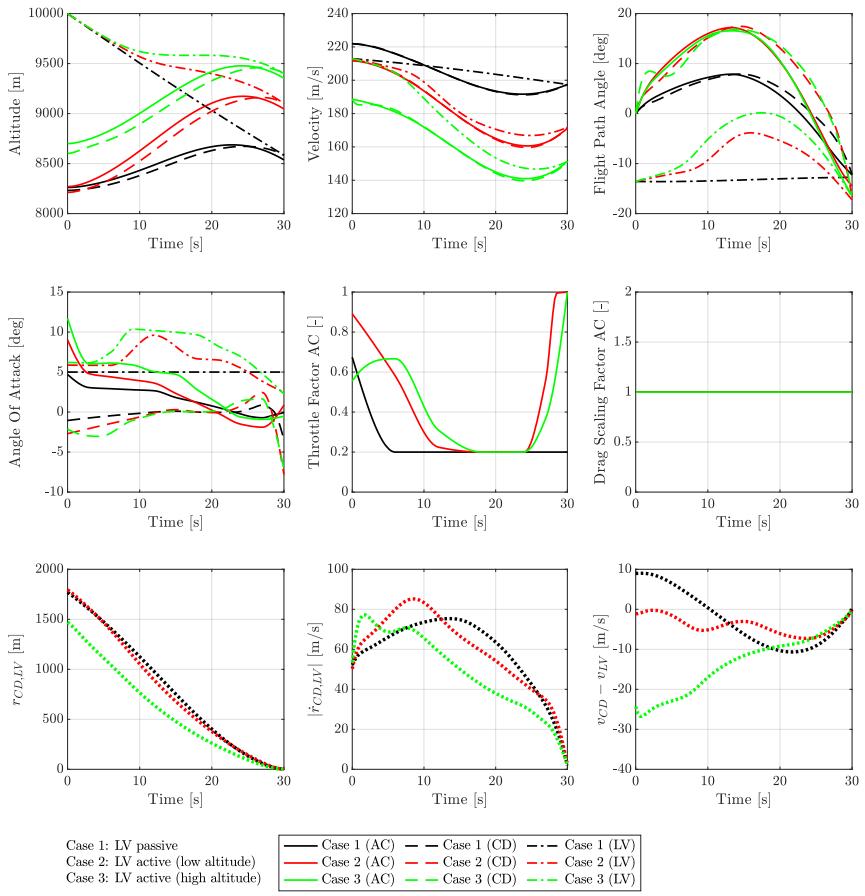

Figure 8: Comparison of the initial capturing maneuvers with a free final launch vehicle flight path angle.

to the launch vehicle. Then, the aircraft performs a pull-up maneuver to steer the capturing device to a rendezvous position. Finally, the alignment to the relatively steep flight path angle of the launch vehicle is realized by a dive of the aircraft. In this scenario, the capturing device remains almost inactive up to the final approach. However, as depicted by the launch vehicle's steep flight path angle and vertical velocity of almost 50 m/s as well as the aircraft's flight path angle and velocity, this initial capturing position is not stable. Consequently, the capturing device will be towed away from the launch vehicle if the capturing attempt is not successful. It should also be noted that the speed of the aircraft increases rapidly at the capturing condition since the throttle scaling factor limit was set to 20 % for the reference case. The initial capturing maneuver can be

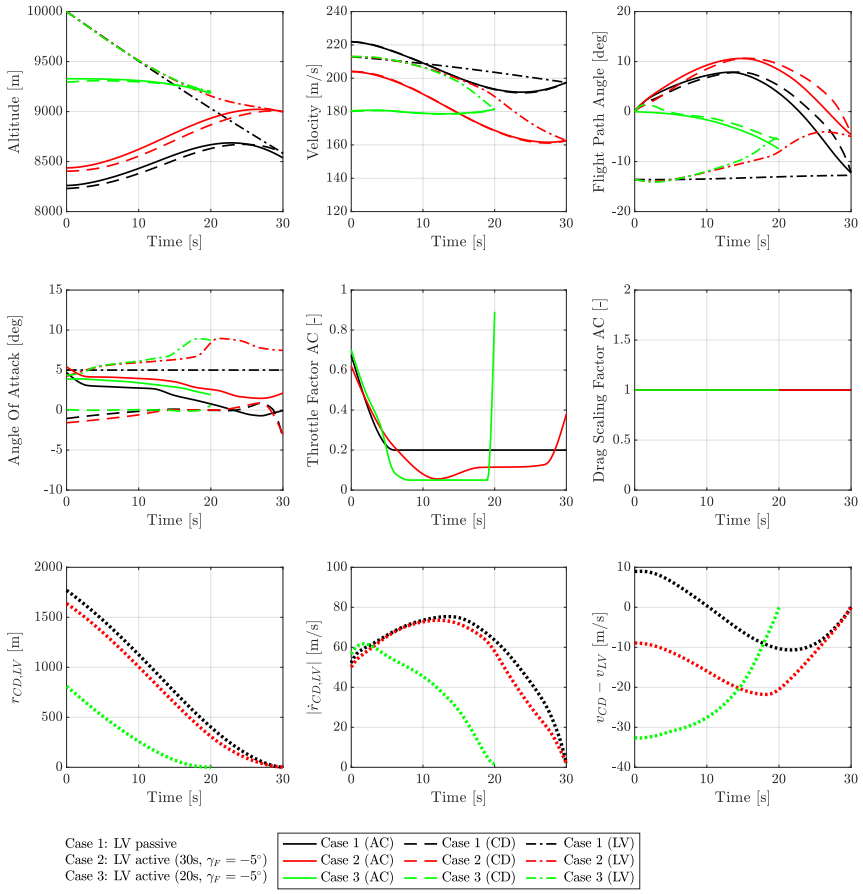

Figure 9: Comparison of the initial capturing maneuvers with a fixed final launch vehicle flight path angle.

performed with shorter or longer overall maneuver time. However, this just causes the initial conditions for the maneuver to change while the quality of the trajectories themselves or the controls remain similar.

A major observation of the scenario with a passive launch vehicle is that an initial in-air-capturing attempt is mathematically feasible, but not sustainable or repeatable in case the initial capturing attempt is unsuccessful. The aim of the remaining studies is to keep the now cooperative launch vehicle at higher altitudes with a shallower flight path angle. For this purpose, an additional constraint for the minimum final altitude of the launch vehicle was introduced to the optimization problem (see Case 2 and Case 3 in Figure 8). Consequently, higher final altitudes and lower final velocities can be achieved for all vehicles.

While the aircraft has to perform more aggressive flight maneuvers, the behavior of the capturing device remains similar. However, at the final capturing approach, large negative flight path angles are obtained for all flight vehicles which are not favorable for multiple recapturing attempts.

To avoid a steep flight path angle, a minimum final flight path angle constraint of $\gamma_F = -5^\circ$ was introduced to the optimization problem. Imposing this constraint on the launch vehicle, the flight path angle of the capturing device is also affected as defined by the capturing conditions. Additionally, the throttle scaling factor limit is decreased to 5 %. As presented in Figure 9, the basic structure of the trajectories remain similar to all previous trajectories in Figure 8, while avoiding highly aggressive control activity as depicted by the angle of attack and the throttle factor. Finally, the same approach was repeated for a flight maneuver with a shorter duration of 20 s to study the influence of a favorable initial line-up of the capturing device and the launch vehicle on the overall trajectory. Consequently, the aircraft is initialized at a higher altitude instantaneously entering a milder dive. However, the controls regarding the throttle factor are slightly more aggressive in order to match the flight path velocity and flight path angle of the launch vehicle as quickly as possible.

Without enforcing a final flight path angle by an optimization constraint, the trajectories with higher final altitude than the reference 'best-glide' configuration show lower final flight path angles which have to be compensated either by aggressive final maneuvering of the aircraft and / or its capturing device. However, the capturing device displays little control activity except at the end of the flight phase to secure the capturing conditions. In general, the highly dynamic control activity can be compensated by adding a final flight path angle constraint for the launch vehicle. Based on the variety of optimized trajectories, the initial in-air-capturing maneuver seems to be feasible from a considerable range of initial relative positions between the launch vehicle and the aircraft. However, to comply with the feasibility requirements regarding redundancy and repeatability of the capturing maneuver, additional studies have been performed focusing on a recapturing maneuver.

4.2. Recapturing Maneuver

In this section, the results of the recapturing maneuver after an initial unsuccessful capturing attempt are evaluated based on the following two scenarios described in Section 4.1. For the passive launch vehicle scenario, the 'best-glide' conditions with a constant angle of attack and a steep flight path angle still apply. However, for initialization the final states of all vehicles after the initial in-air-capturing attempt are used. For the cooperative launch vehicle scenario, the vehicles are initialized using the final states obtained from the initial in-air-capturing maneuver for the case with a fixed final flight path angle. For both cases, the main optimization goal is to reach the favorable capture conditions as fast as possible, which can be achieved under certain conditions within 5 s. For all cases, the engines are throttled back to the minimum allowable value. The drag scaling factor of the aircraft is active and must be increased to significant levels to comply with the favorable capturing conditions.

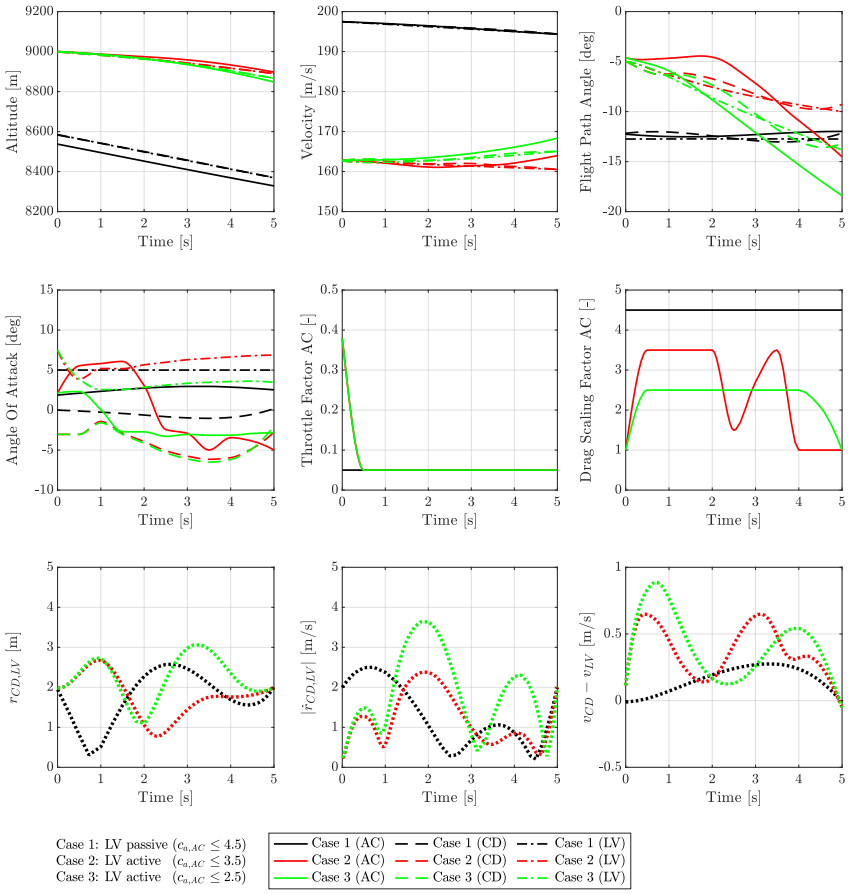

Figure 10: Comparison of the recapturing maneuvers.

The drag scaling factor is especially relevant for the scenario with a passive launch vehicle as shown in Figure 10. In order to satisfy the capturing conditions stated in Table 4, it is necessary to use a drag scaling factor of 4.5 which is way above what is achievable by air brake systems usually installed on commercial airplanes. In this case, the aircraft must be significantly modified with additional and improved air brake systems capable of adapting the lift-to-drag ratio of the aircraft to the launch vehicle's lift-to-drag ratio. Alternatively, a side-slip maneuver could be performed to generate the necessary drag. However, due to the lack of aerodynamic data, the side-slip maneuver was not considered in this study. Using a passive launch vehicle and a drag scaling factor of 4.5 for the aircraft, the capturing device can be kept near to the launch vehicle during the complete recapturing attempt.

For the recapturing scenario with a cooperative launch vehicle, the maximum allowable drag scaling factor is reduced to 3.5 for Case 2 and to 2.5 for Case 3 as shown in Figure 10. With a maximum drag scaling factor of 2.5, a recapturing attempt is barely possible since the final conditions after the recapturing attempt are not favorable for further flight phases. In particular, the final flight path angle of the cooperative launch vehicle is at the level achieved by the recapturing attempt with a passive launch vehicle. Furthermore, the relative velocity of the aircraft with respect to the launch vehicle increases continuously, while the aircraft loses altitude. Therefore, a third recapturing attempt would be infeasible.

The drag scaling limit of 3.5 results in more favorable capturing conditions with a final flight path angle of the launch vehicle around $-10°$. Additionally, the launch vehicle and the aircraft show similar altitude losses. However, the aircraft's velocity still increases significantly with respect to the launch vehicle. This increase in the relative velocity can be explained by the reduction of the drag scaling factor at the end of the trajectory optimization. Adjusting the flight duration limits for further optimizations would possibly reduce the final relative velocities.

Accordingly, a recapturing attempt after an unsuccessful initial in-air-capturing approach is possible under certain conditions. For a passive launch vehicle, the overall aerodynamic drag of the aircraft must be adjustable up to 4.5 times its nominal drag in a short period of time. This would require the aircraft to be significantly modified according to the requirements of the in-air-capturing maneuver. Although this applies to both the passive and the active launch vehicle scenarios, the required overall drag scaling of the aircraft would decrease with higher maneuverability of the unpowered launch vehicle. Additionally, the capturing device shows more control activity and agility during the recapturing attempt compared to the initial in-air-capturing maneuver. Finally, for a cooperative launch vehicle, the final flight path angle after the first capturing maneuver should be targeted at $-5°$ up to $-10°$ to enable further recapturing attempts. Under these conditions the cooperative launch vehicle can fly at larger altitudes after an initial capture at a lower velocity which could allow for multiple subsequent capturing attempts.

5. Conclusion

The objective of this paper was to introduce the modeling and simulation framework for the in-air-capturing scenario involving multiple flight vehicles and to present the trajectory optimization results of the in-air-capturing maneuver in order to assess its feasibility. First, the object-oriented and equation-based modeling language Modelica and the in-air-capturing multibody model including multiple flight vehicles were presented. Then, the trajectory optimization results were discussed for an initial in-air-capturing maneuver and a subsequent recapturing maneuver assuming an unsuccessful first capturing attempt.

The overall results show that an initial in-air-capturing attempt for the setup with a passive launch vehicle is feasible under certain conditions. However,

for a successful in-air-capturing maneuver with minimum control efforts and multiple recapturing attempts, an actively controlled aircraft with advanced drag-increasing air brake systems and a cooperative launch vehicle maintaining a reasonable flight path angle are required.

To conclude, these reference trajectories can be used for controllability studies and control system design with 6-DOF flight dynamics models considering a flexible cable, time delays, disturbances, and uncertainties. Within future trajectory optimizations, the aerodynamic bank angle constraint of the launch vehicle will be removed to study the influence of rolling maneuvers during approach. Furthermore, the major modifications required for the aircraft in terms of drag-increasing air brake systems will be evaluated.

Acknowledgements

This study was performed within the DLR internal project AKIRA. The authors would like to thank their colleagues at DLR's Institute of Space Systems (RY) and its *Space Launcher System Analysis* department for providing data for the flight vehicles involved in the in-air-capturing maneuver. Especially, the authors would like to thank their former colleague Dr. Klaus Schnepper at DLR's Institute of System Dynamics and Control (SR) for his insightful comments and important contributions to the trajectory optimization of the in-air-capturing maneuver.

Declaration of Interest

The authors declare that they have no competing interests.

References

[1] M. Sippel, J. Klevanski, J. Kauffmann, Innovative Method for Return to the Launch Site of Reusable Winged Stages, in: 52nd International Astronautical Congress, 2001.

[2] J. Klevanski, A. Herbertz, M. Sippel, J. Kauffmann, Verfahren zum Bergen einer Stufe eines mehrstufigen Raumtransportsystems, patent DE10147144C1 (2001).

[3] M. Sippel, S. Stappert, J. Wilken, N. Darkow, S. Cain, S. Krause, T. Reimer, C. Rauhe, D. Stefaniak, M. Beerhorst, T. Thiele, R. Kronen, L. E. Briese, P. Acquatella B., K. Schnepper, J. Riccius, Focused research on RLV-technologies: the DLR project AKIRA, in: 8th European Conference for Aeronautics and Space Sciences (EUCASS), 2019.

[4] L. Bussler, M. Sippel, Comparison of Return Options for Reusable First Stages, in: 21st AIAA International Space Planes and Hypersonics Technologies Conferences, 2017.

[5] M. Sippel, S. Stappert, L. Bussler, E. Dumont, Systematic Assessment of Reusable First-Stage Return Options, in: 68th International Astronautical Congress, 2017.

[6] SpaceX, Falcon User's Guide (2019).

[7] Blue Origin, New Glenn Payload User's Guide, revision C (2018).

[8] D. R. Jenkins, Space Shuttle: The History of the National Space Transportation System - The First 100 Missions, 2010, 3rd Edition.

[9] M. Sippel, J. Klevanski, Progresses in Simulating the Advanced In-Air-Capturing Method, in: 5th International Conference on Launcher Technology, 2003.

[10] M. Sippel, J. Klevanski, Preliminary Definition of an Aerodynamic Configuration for a Reusable Booster Stage within Tight Geometric Constraints, in: Proceedings of the 5th European Symposium on Aerothermodynamics for Space Vehicles, 2004.

[11] M. Sippel, J. Klevanski, Simulation of Dynamic Control Environments of the In-Air-Capturing Mechanism, in: 6th International Symposium on Launcher Technology, 2005.

[12] L. E. Briese, K. Schnepper, P. Acquatella B., Multi-Disciplinary Modeling Environment for Reusable Launch Vehicle Dynamics and Control System Design, in: 8th European Conference for Aeronautics and Aerospace Sciences (EUCASS), 2019.

[13] S. Cain, S. Krause, J. Binger, Entwicklung einer automatischen Koppeleinheit für das Einfangen einer wiederverwendbaren Trägerstufe im In-Air-Capturing, in: Deutscher Luft- und Raumfahrtkongress, 2017.

[14] S. Cain, S. Krause, J. Binger, First Development Steps of an Actively Controlled Drogue, in: International Conference on Unmanned Aircraft Systems, 2018.

[15] M. Sippel, L. Bussler, S. Krause, S. Cain, S. Stappert, Bringing Highly Efficient RLV-Return Mode 'In-Air-Capturing' to reality, in: HiSST: International Conference on High-Speed Vehicle Science Technology, 2018.

[16] M. Sippel, S. Stappert, L. Bussler, S. Krause, S. Cain, Highly Efficient RLV-Return Mode 'In-Air-Capturing' Progressing by Preparation of Subscale Flight Tests, in: 8th European Conference for Aeronautics and Space Sciences (EUCASS), 2019.

[17] Modelica Association, Modelica - A Unified Object-Oriented Language for Physical Systems Modeling, Language Specification Version 3.4 (2017).

[18] P. Fritzson, P. Bunus, Modelica - A General Object-Oriented Language for Continuous and Discrete-Event System Modeling and Simulation, in: 35th Annual Simulation Symposium, 2002.

[19] H. Elmqvist, S. E. Mattsson, M. Otter, Modelica - An International Effort to Design an Object-Oriented Modeling Language, in: Summer Computer Simulation Conference, 2003.

[20] DYMOLA, Version 2018, Vélizy-Villacoublay, France, Dassault Systèmes, 2018.

[21] L. E. Briese, K. Schnepper, P. Acquatella B., Advanced Modeling and Trajectory Optimization Framework for Reusable Launch Vehicles, in: IEEE Aerospace Conference, 2018.

[22] L. E. Briese, P. Acquatella B., K. Schnepper, Multidisciplinary modeling and simulation framework for launch vehicle system dynamics and control, Acta Astronautica 170. doi:10.1016/j.actaastro.2019.08.022.

[23] G. Looye, The New DLR Flight Dynamics Library, in: Proceedings of the 6th International Modelica Conference, 2008.

[24] A. Klöckner, G. Looye, R. Müller, R. Kuchar, F. Re, M. Leitner, Object-Oriented Aircraft Modeling with the DLR FlightDynamics library, in: 9th AIRTEC 2014 International Congress, 2014.

[25] M. J. Reiner, J. Bals, Nonlinear inverse models for the control of satellites with flexible structures, in: Proceedings of the 10th International Modelica Conference, 2014. doi:10.3384/ecp14096577.

[26] M. J. Reiner, J. G. Fernandez, G. Ortega, Combined Control for Active Debris Removal using a Satellite Equipped with a Robot Arm, in: 10th International ESA Conference on Guidance, Navigation and Control Systems (ESA GNC), 2017.

[27] P. Acquatella B., M. J. Reiner, Modelica Stage Separation Dynamics Modeling for End-to-End Launch Vehicle Trajectory Simulations, in: Proceedings of the 10th International Modelica Conference, 2014. doi:10.3384/ecp14096589.

[28] M. Otter, H. Elmqvist, S. E. Mattsson, The New Modelica MultiBody Library, in: Proceedings of the 3rd International Modelica Conference, 2003.

[29] L. E. Briese, A. Klöckner, M. J. Reiner, The DLR Environment Library for Multi-Disciplinary Aerospace Applications, in: Proceedings of the 12th International Modelica Conference, 2017. doi:10.3384/ecp17132929.

[30] F. G. Lemoine, S. C. Kenyon, J. K. Factor, R. G. Trimmer, N. K. Pavlis, D. S. Chinn, C. M. Cox, S. M. Klosko, S. B. Luthcke, M. H. Torrence, Y. M. Wang, R. G. Williamson, E. C. Pavlis, R. H. Rapp, T. R. Olson, The Development of the Joint NASA GSFC and National Imagery and Mapping Agency NIMA Geopotential Model EGM96, Tech. rep., National Aeronautics and Space Administration (NASA) (1998).

[31] NASA, U.S. Standard Atmosphere, 1976, Tech. rep., National Aeronautics and Space Administration (NASA) (1976).

[32] P. Acquatella B., L. E. Briese, K. Schnepper, Guidance command generation and nonlinear dynamic inversion control for reusable launch vehicles, Acta Astronautica 174. doi:10.1016/j.actaastro.2020.04.002.

[33] M. Sippel, O. Trivailo, L. Bussler, S. Lipp, C. Valluchi, Evolution of the SpaceLiner towards a Reusable TSTO-Launcher, in: 67th International Astronautical Congress, 2016.

[34] M. Sippel, C. Valluchi, L. Bussler, A. Kopp, N. Garbers, S. Stappert, S. Krummen, J. Wilken, SpaceLiner Concept as Catalyst for Advanced Hypersonic Vehicles Research, in: 7th European Conference for Aeronautics and Space Sciences (EUCASS), 2017.

[35] S. Krause, S. Cain, G. Strikert, L. Bussler, S. Stappert, FALCon - Formation Flight for In-Air Launcher 1st Stage Capturing Demonstration - Scaled Experiment Scenario Description, Tech. rep., DLR German Aerospace Center (2020).

[36] H.-D. Joos, J. Bals, G. Looye, K. Schnepper, A. Varga, A multi-objective optimisation-based software environment for control systems design, in: IEEE International Symposium on Computer Aided Control System Design Proceedings, 2002.

[37] H.-D. Joos, MOPS - Multi-Objective Parameter Synthesis, Tech. Rep. DLR-IB-SR-OP-2016-128, DLR German Aerospace Center (2016).

[38] K. Schnepper, Trajektorienoptimierung in MOPS - Das Paket trajOpt Version 1.0, Tech. rep., DLR German Aerospace Center (2014).

[39] Modelica Association, Functional Mock-Up Interface for Model Exchange and Co-Simulation (2015).